REPORT DOCUMENTATION PAGE

Form Approved OMB NO. 0704-0188

1. REPORT DATE (DD-MM-YYYY)	2. REPORT TYPE	3. DATES COVERED (From - To)
01-02-2017	Final Report	1-Sep-2015 - 31-May-2016

4. TITLE AND SUBTITLE
Final Report: Electrode-Specific Molecular Wires for Bioelectrochemical Systems (Chemical Sciences)

5a. CONTRACT NUMBER
W911NF-15-1-0486

5b. GRANT NUMBER

5c. PROGRAM ELEMENT NUMBER
611102

6. AUTHORS
Guillermo Bazan

5d. PROJECT NUMBER

5e. TASK NUMBER

5f. WORK UNIT NUMBER

7. PERFORMING ORGANIZATION NAMES AND ADDRESSES
University of California - Santa Barbara
3227 Cheadle Hall
3rd floor, MC 2050
Santa Barbara, CA 93106 -2050

8. PERFORMING ORGANIZATION REPORT NUMBER

9. SPONSORING/MONITORING AGENCY NAME(S) AND ADDRESS (ES)
U.S. Army Research Office
P.O. Box 12211
Research Triangle Park, NC 27709-2211

10. SPONSOR/MONITOR'S ACRONYM(S)
ARO

11. SPONSOR/MONITOR'S REPORT NUMBER(S)
63692-CH-II.1

12. DISTRIBUTION AVAILIBILITY STATEMENT
Approved for Public Release; Distribution Unlimited

13. SUPPLEMENTARY NOTES
The views, opinions and/or findings contained in this report are those of the author(s) and should not contrued as an official Department of the Army position, policy or decision, unless so designated by other documentation.

14. ABSTRACT
Conjugated oligoelectrolytes (COE's) are molecules defined by a conjugated, semi-conducting backbone and pendant ionic functionalities which afford solubility in polar solvents – a feature which has allowed for the utilization of these molecules in biological systems. Through interactions with microbial membranes, certain classes of COE's have been shown to improve the performance of bioelectrochemical devices such as microbial fuel cells (MFC's). To this point, the use of COE's in microbial devices has been limited to the addition of solutions of the synthetic compounds to suspensions of cells. Instead of directly influencing the microbes, the aim

15. SUBJECT TERMS
Conjugated oligoelectrolytes, microbial fuel cells, self-assembled monolayers, biotic-abiotic interfaces

16. SECURITY CLASSIFICATION OF:			17. LIMITATION OF ABSTRACT	15. NUMBER OF PAGES	19a. NAME OF RESPONSIBLE PERSON
a. REPORT	b. ABSTRACT	c. THIS PAGE			Guillermo Bazan
UU	UU	UU	UU		19b. TELEPHONE NUMBER 805-893-5538

Report Title

Final Report: Electrode-Specific Molecular Wires for Bioelectrochemical Systems (Chemical Sciences)

ABSTRACT

Conjugated oligoelectrolytes (COE's) are molecules defined by a conjugated, semi-conducting backbone and pendant ionic functionalities which afford solubility in polar solvents – a feature which has allowed for the utilization of these molecules in biological systems. Through interactions with microbial membranes, certain classes of COE's have been shown to improve the performance of bioelectrochemical devices such as microbial fuel cells (MFC's). To this point, the use of COE's in microbial devices has been limited to the addition of solutions of the synthetic compounds to suspensions of cells. Instead of directly influencing the microbes, the aim of this study was to modify the anode of a MFC in order to enhance physical and electronic interactions at the biotic-abiotic interface. To achieve the electrode modification, a novel COE containing a terminal thiol was designed and synthesized. Formation of self-assembled monolayers through thiolate-gold bonds was confirmed by X-ray photoelectron spectroscopy. Increase physical interaction between bacterial cells and gold films as a result of surface modification was observed by scanning electron microscopy. Microbial fuel cells utilizing gold electrodes functionalized with this molecule showed a 27% increase in current generation and an 81% increase in peak power relative to bare gold electrodes.

Enter List of papers submitted or published that acknowledge ARO support from the start of the project to the date of this printing. List the papers, including journal references, in the following categories:

(a) Papers published in peer-reviewed journals (N/A for none)

Received Paper

TOTAL:

Number of Papers published in peer-reviewed journals:

(b) Papers published in non-peer-reviewed journals (N/A for none)

Received Paper

TOTAL:

Number of Papers published in non peer-reviewed journals:

(c) Presentations

Number of Presentations: 0.00

Non Peer-Reviewed Conference Proceeding publications (other than abstracts):

Received Paper

TOTAL:

Number of Non Peer-Reviewed Conference Proceeding publications (other than abstracts):

Peer-Reviewed Conference Proceeding publications (other than abstracts):

Received Paper

TOTAL:

Number of Peer-Reviewed Conference Proceeding publications (other than abstracts):

(d) Manuscripts

Received Paper

TOTAL:

Number of Manuscripts:

Books

Received Book

TOTAL:

Received	Book Chapter

TOTAL:

Patents Submitted

Patents Awarded

Awards

Graduate Students

NAME	PERCENT_SUPPORTED	Discipline
Alex Moreland	0.46	
FTE Equivalent:	**0.46**	
Total Number:	**1**	

Names of Post Doctorates

NAME	PERCENT_SUPPORTED
FTE Equivalent:	
Total Number:	

Names of Faculty Supported

NAME	PERCENT_SUPPORTED	National Academy Member
Guillermo Bazan	0.00	
FTE Equivalent:	**0.00**	
Total Number:	**1**	

Names of Under Graduate students supported

NAME	PERCENT_SUPPORTED
FTE Equivalent:	
Total Number:	

Student Metrics

This section only applies to graduating undergraduates supported by this agreement in this reporting period

The number of undergraduates funded by this agreement who graduated during this period: 0.00

The number of undergraduates funded by this agreement who graduated during this period with a degree in science, mathematics, engineering, or technology fields:..... 0.00

The number of undergraduates funded by your agreement who graduated during this period and will continue to pursue a graduate or Ph.D. degree in science, mathematics, engineering, or technology fields:..... 0.00

Number of graduating undergraduates who achieved a 3.5 GPA to 4.0 (4.0 max scale):..... 0.00

Number of graduating undergraduates funded by a DoD funded Center of Excellence grant for Education, Research and Engineering:..... 0.00

The number of undergraduates funded by your agreement who graduated during this period and intend to work for the Department of Defense 0.00

The number of undergraduates funded by your agreement who graduated during this period and will receive scholarships or fellowships for further studies in science, mathematics, engineering or technology fields: 0.00

Names of Personnel receiving masters degrees

NAME

Total Number:

Names of personnel receiving PHDs

NAME

Total Number:

Names of other research staff

NAME PERCENT_SUPPORTED

FTE Equivalent:
Total Number:

Sub Contractors (DD882)

Inventions (DD882)

Scientific Progress

See Attachment.

Technology Transfer

Electrode-Specific Molecular Wires for Bioelectrochemical Systems

Guillermo C. Bazan, University of California

Paramount to the success of emerging bioelectrochemical technologies is better understanding and control of biotic-abiotic interfaces. Of particular importance for furthering technologies, such as waste-water remediation, energy generation and biolelectroysnthesis, is the electronic communication between microbes and charge collecting (or injecting) external electrodes. The goal of the STIR grant described herein is to address two critical factors involved in the transfer of electrons between microbes and electrodes – the physical proximity of the biotic and abiotic components and the ability to transfer charge across the cell membrane. Previous work in our group demonstrated the ability of conjugated oligoelectrolytes (COEs) to spontaneously intercalate into cell membranes and subsequently enhance the electronic connection between microbes and an electrode. The synthetic target of this project is a modified COE molecule, which incorporates a specific functionality for electrode surface functionalization. In this manner, we hope to simultaneously improve electron motion through the cell membrane and tether the microbes directly to the electrode.

The path of this study can be divided into five distinct sections, each with a major milestone goal as follows: 1) the design and synthesis of the aforementioned surface-binding COE molecule, 2) confirmation and optimization of the COE self-assembled monolayer (SAM) on an electrode, 3) verification of the ability of the COE to spontaneously intercalate into bacterial membranes, 4) confirmation that the COE SAM promotes physical cell-electrode interactions, and 5) demonstration of the ability of this system to increase electronic communication between the cells and the electrode. These five goals are depicted in Figure 1 below. As described in more detail below, the synthesis of these molecules has little precedent in the literature and constitutes in their own right a significant chemistry-centric challenge. Despite the need to carve new synthetic strategies, we are pleased to state that all goals were successfully achieved.

Figure 1: Depiction of Five Milestones as they apply to the Overall Project Goal

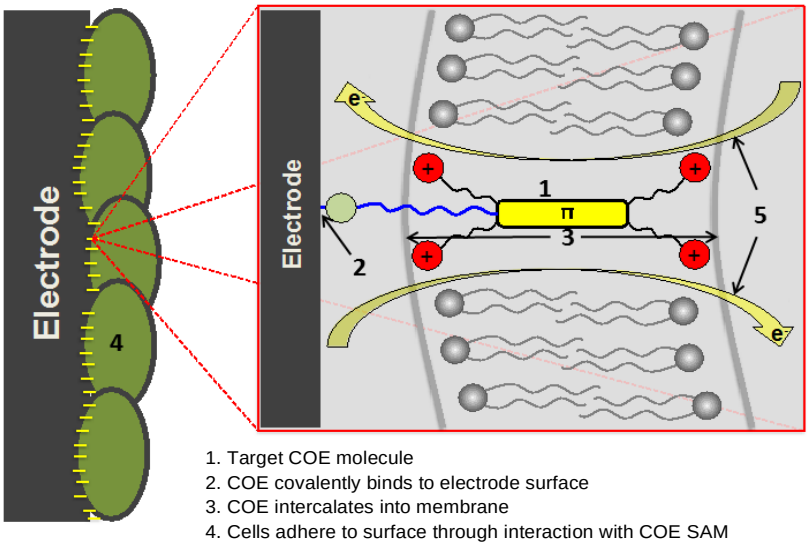

1. Target COE molecule
2. COE covalently binds to electrode surface
3. COE intercalates into membrane
4. Cells adhere to surface through interaction with COE SAM
5. COE increases cell-electrode electronic communication

The modularity of COE design is summarized in Figure 2. The phenylene-vinyl core may consist of different numbers of repeat units and the pendant R-groups can vary in substitution position, as well as chemical composition. In our previously reported COEs, R-groups are identical on both termini of the molecule. As an example, DSSN+ (shown in Figure 3) is the molecule where *n* = 2 and the pendant groups are trimethylammonium-terminated amino linkages at the *para*-position. In designing the target molecule for this study, the first consideration was the backbone length. Recent work demonstrated that COEs with *n* = 2 typically show the lowest toxicity and the highest electrochemical enhancement. As such, only COEs with the 4-ring backbone will be described in this study. Additionally, these COEs will only contain 3,5-dialkoxy linkages for reasons related to the reactivity and stability of intermediates. Specifically, the presence of amine functionalities renders certain intermediates prone to oxidation. Finally, the R1-group of these COEs will contain a thiol functionality due to the strong literature precedent for forming monolayers on gold surfaces through gold-sulfur bonds.

Scheme 1 outlines the proposed pathway to the initial target molecule. Similar to the manner in which our previously report COEs were synthesized, the phenylene-vinylene core of this target molecule was accessed through the Horner-Wadsworth-Emmons Reaction. In the case of the symmetrical COEs, two equivalents of molecule **1** would be reacted with molecule **2** to yield the core in a single step. For the target molecule of this project, this tandem reaction is divided into two sequential reactions (*ia.* and *ib.*) in order

Figure 2: Chemical Design Overview

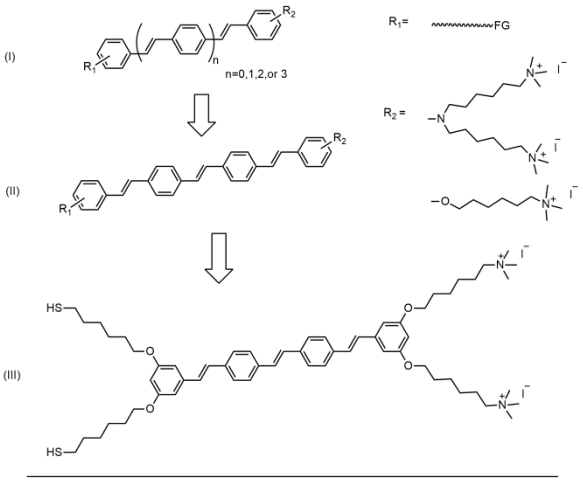

(I) General phenylenevinylene-based COE structure
(II) 4-ring backbone selected for this study based on low toxicity
(III) Alkoxy linkages and thiol functionalities selected for this study

Figure 3: Previously Reported COEs

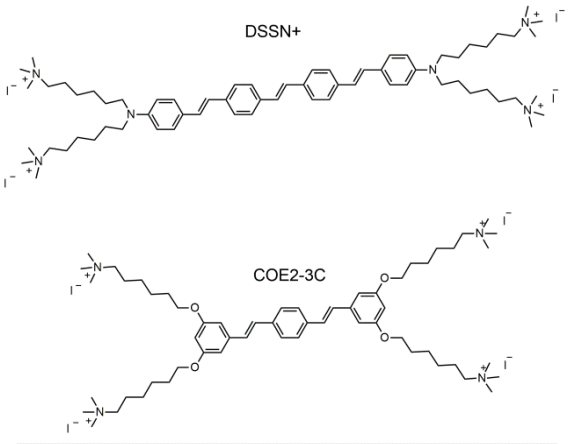

to introduce asymmetry. Molecule **2** first undergoes a reaction with a single equivalent of molecule **1**. This intermediate **3** then undergoes an analogous reaction with one equivalent of molecule **4**, itself a derivative of molecule **1**. This method is a critical component of the synthesis of every COE designed for this study. In the initial pathway descrived in Scheme 1, very limited conversion was achieved for reaction *ib.*, despite a wide variety of conditions screened. Ultimately, a small amount of molecule **5** was obtained using *n*-butyl lithium and sequential addition of molecules **3** and **4**. Molecule **5** was subsequently reacted with trimethylamine to afford molecule **6**. An attempt to functionalize a gold surface with this molecule was unsuccessful based on the XPS spectrum shown in Figure 4. The fact that that no thiolate-gold bond was formed is evident in the energy associated with the S 2p peak – thiolate-gold bonds generally appear in the region of 159-162eV, while the peak observed at 164eV is more typical of a thioacetate.

Scheme 1: Initial Steps Toward Proposed Molecule

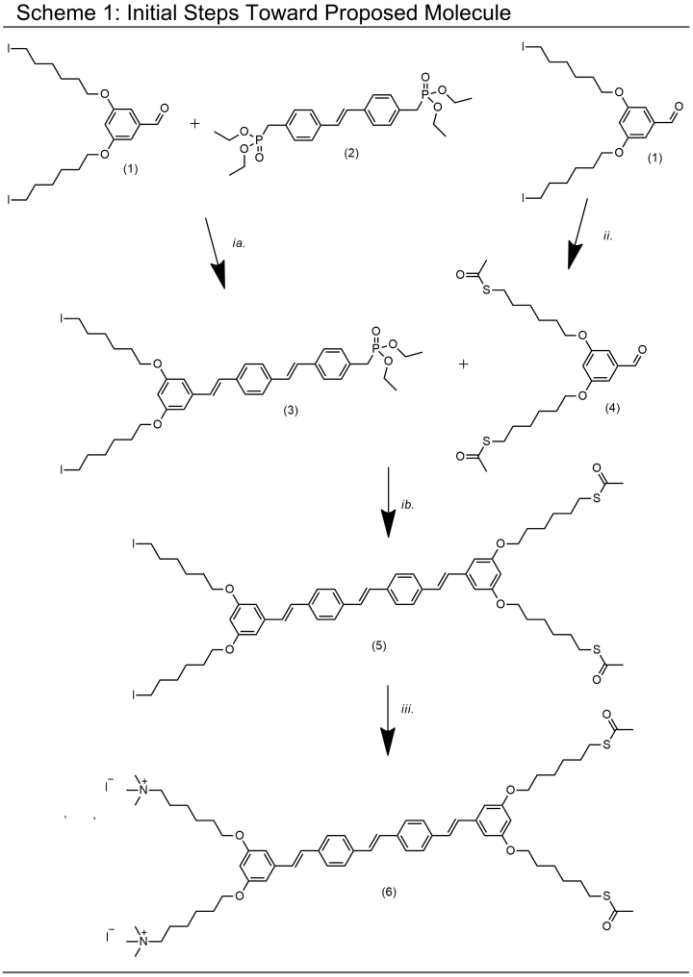

ia. NaOtBu, THF, RT 16h, 52%; *ii.* KSAc, MEK, reflux 12h, 99%; *ib.* base, THF, various conditions, 0-30%; *iii.* TMA, THF/MeOH, RT 2d, 93%

Figure 4: XPS Spectrum of Molecule **6** on Gold Substrate

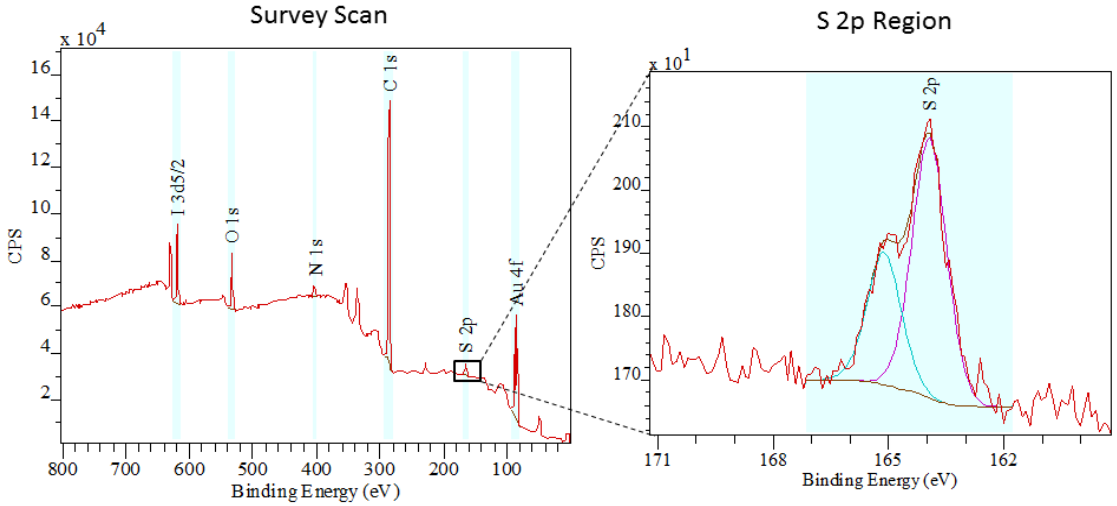

XPS sample prepared by immersing gold-coated substrate in 40mM solution of **6** in dichloromethane and methanol for 18 hours

The carbon, nitrogen, oxygen, and iodine signals indicate that molecule **6** is on the substrate. However, without an apparent thiolate-gold signal, these peaks can be attributed to physical adsorption of the molecule. This adsorption is likely facilitated by strong interactions between the pi-conjugated backbone of molecule **6** and the gold surface.

The difficulties with reaction *ib.* in Scheme 1 may be due to a reaction between the thioacetate functionalities and the ylide intermediate generated during the Horner-Wadsworth-Emmons reaction. In an attempt to circumvent this issue, three analogues of molecule **4** were synthesized – the free-thiol **4'**, the potassium thiolate salt **4''**, and the MOM-protected thiol **4'''**. The thiols were readily oxidized to disulfides during the course of reaction *ib*. The thiolate salt was unstable, possibly due to a reaction between the nucleophilic thiolate and the electrophilic aldehyde. The MOM-protected thiol was stable to the conditions of reaction *ib* but subsequent de-protection efforts were unsuccessful.

Figure 5: Analogues of Molecule **4**

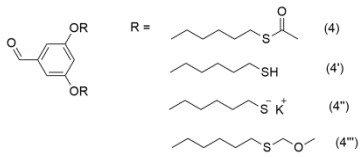

Due to the functional group compatibility problems described above, a revised synthesis was devised that incorporates the sulfur-containing functionality at a later stage (Scheme 2). Additionally, this revised synthesis targets a molecule with a bridging ammonium group between the sulfur and the core. The new target molecule was expected to have greater solubility, resemble traditional COEs more closely, and allow more space between substrate and the cell membrane in order to better accommodate transmembrane proteins. The scheme also allows for modularity with respect to the distance between the substrate and the bridging ammonium. Unfortunately, the intermediate following reaction *v.* was insoluble in solvents appropriate for halogen exchange (reaction *vi*.) and compound **9** was not accessible by this route. A minor modification was made in an attempt to preserve solubility. In Scheme 3, the route proceeds through intermediates with one charge (molecules

Scheme 2: Route to improved molecule

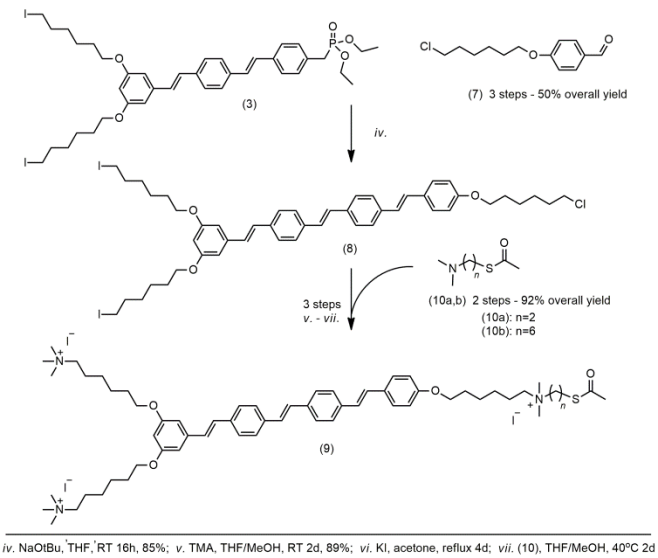

iv. NaOtBu, THF, RT 16h, 85%; *v*. TMA, THF/MeOH, RT 2d, 89%; *vi*. KI, acetone, reflux 4d; *vii*. (10), THF/MeOH, 40ºC 2d

15 and **16**) rather than two charges as in Scheme 2. The key to the success of this route is the solubility of intermediate **15**, which allowed for efficient halogen exchange in reaction *xi*. Following step *xii.*, initial attempts to de-protect the thioacetate in molecule **17** proved unsuccessful. The mass spectrum of molecule **17** revealed that a significant fraction of the sample existed as the disulfide dimer (**17b**). It was eventually determined that dimers were formed through de-protection and subsequent oxidation of the sulfur atom during the course of reaction *xii*. This quaternization step calls for methanol in order to maintain solubility as more ionic functionalities are added to the molecule. Methanol alone is not known to de-protect thioacetates but in the presence of trimethylamine, a small portion of methoxide ions can be formed. These methoxide ions can remove the acetate group, producing methylacetate and a thiolate, which can subsequently acquire a proton. As tertiary amines are known to oxidize thiols to disulfides, any thiol formed during the reaction would rapidly dimerize with another thiol due to the trimethylamine in the reaction. Given that disulfides are known to form gold-thiolate monolayers, albeit more slowly than thiols, an attempt was made to functionalize a gold surface with the mixture of molecule **17** and the corresponding disulfide dimers. Similar to the results with molecule **6**, XPS analysis indicated that molecule **17** only interacted with the gold surface by physical absorption. It became apparent that forming the free thiol was critical to the successful formation of gold-thiolate bonds. Efforts were thus made to determine appropriate conditions for both deprotection and disulfide reduction of molecule **17** and the

Scheme 3:

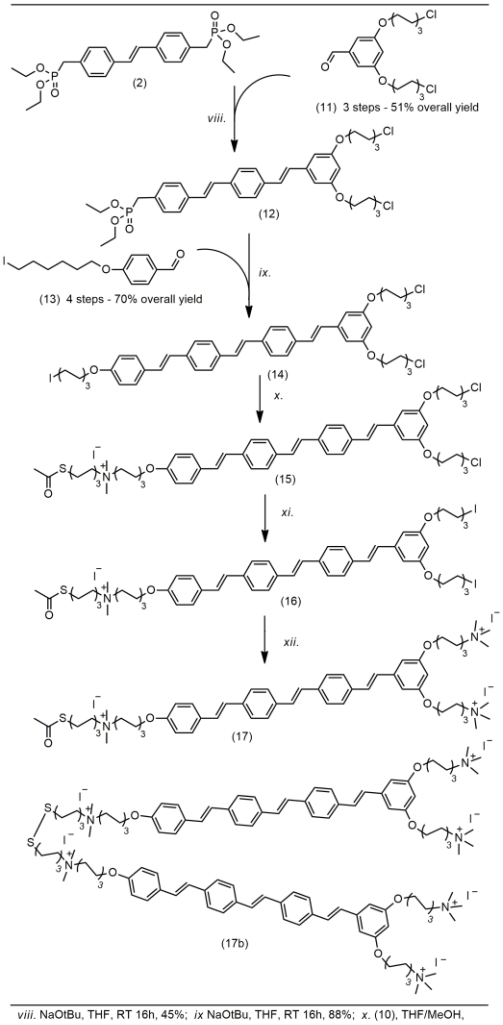

viii. NaOtBu, THF, RT 16h, 45%; *ix* NaOtBu, THF, RT 16h, 88%; *x*. (10), THF/MeOH, 40°C 3d, 79%; *xi*. KI, acetone, reflux 4d, 80%; *xii*. TMA, THF/MeOH, 40°C 2d, 75%

Concurrent with the efforts to synthesize the free thiol analogue of molecule 17, a new method for SAM preparation was devised and tested. The two-step process involves first functionalizing the gold surface with a thiol molecule containing a terminal tertiary amine. This amine could then quaternize with the alkyl-iodide functionality of a COE precursor. An outline of this method can be seen below in Figure 6. Starting from the previously-synthesized molecule **10b**, a free-thiol analogue was synthesized to facilitate better SAM formation (molecule **18b** in Scheme 4). Importantly, this de-

Scheme 4:

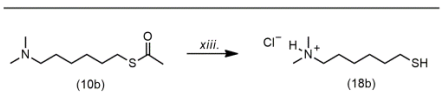

xiii. HCl, MeOH, 40°C 24h, 85%

protection with hydrochloric acid also resulted in the formation of the hydrochloride adduct of the tertiary amine which prevented interactions between the amine and the thiol functionalities. Upon treating a gold surface with this molecule, a bilayer was observed by XPS. This hydrogen-bonding behavior in nitrogen-containing molecules is known in the literature. Additionally, gold-nitrogen interactions were observed. In order to form the tertiary amine and remove the top layer, the sample was treated with potassium carbonate in methanol. As a model compound, molecule **14** was used for the quaternization step. Based on XPS, the desired final monolayer was not achieved, either as a result of the inability to efficiently disrupt the bilayer or difficulty with the quaternization step.

Figure 6: Multi-Step Approach to COE Monolayer Formation

a. formation of hydrogen-bonded bilayer containing tri-alkyl ammonium hydrochloride salts

b. base-treatment to produce a monolayer with terminal tertiary amine functionalities

c. quaternization reaction with alkyl-iodide functionality of COE precursor

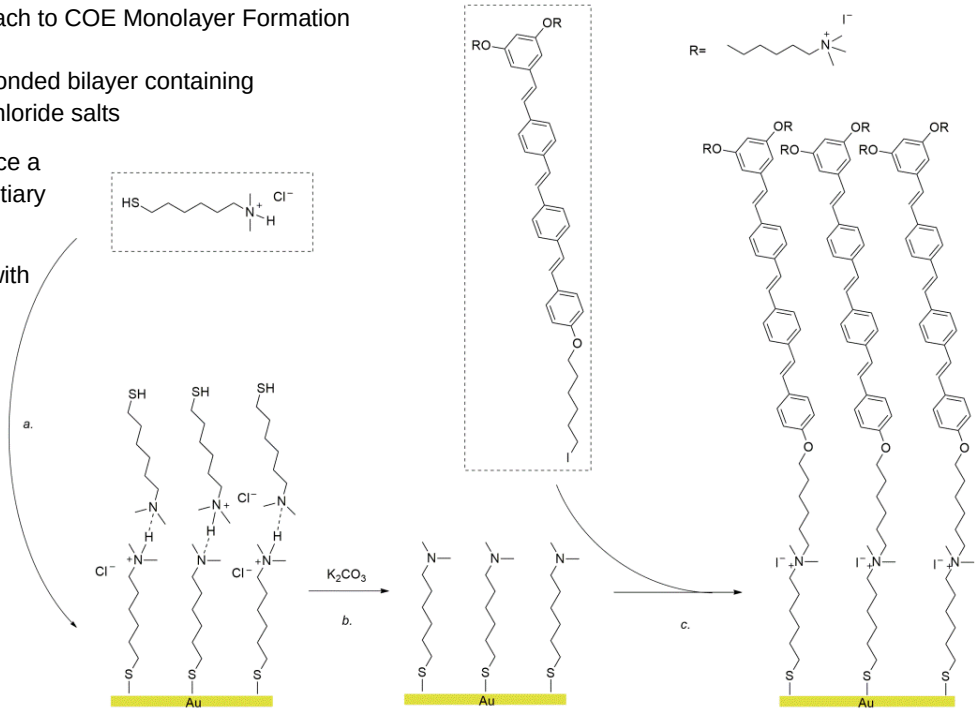

To further explore this two-step pathway to SAM formation, a new set of molecules was designed and synthesized (Scheme 5). Instead of initially forming an amine-terminated SAM, an alkyl thiol with a terminal azide (molecule **24**) was synthesized and used to functionalize the gold surface. A COE molecule with a terminal alkyne (molecule **28**) was synthesized such that linking the COE to the pre-formed SAM could be achieved through copper-catalyzed azide-alkyne cycloaddition (Figure 7a-b). XPS confirmed the presence of the sulfur-gold bond and the azide following the initial SAM formation (Figure 7c-d). The azide peaks also provide a convenient means to monitor the subsequent cycloaddition reaction as the triazole product has a different N 1s binding energy. XPS confirmation of the cycloaddition (Figure 7e) has proven that this approach can be used to successfully form COE monolayers on gold.

Scheme 5: Synthesis of Cycloaddition Partners

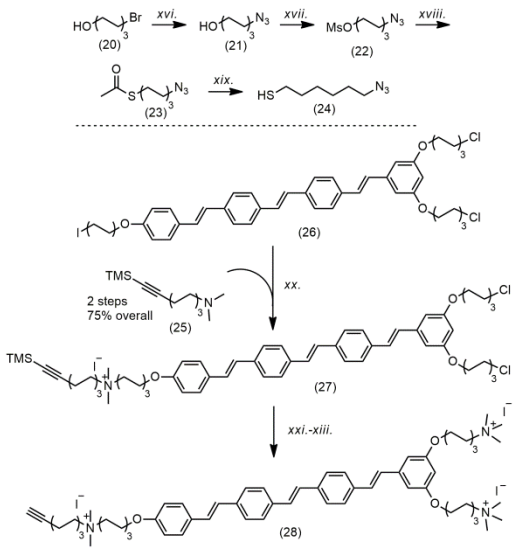

xvi. NaN_3, DMF, 80°C 24h, 85%; *xvii.* MsCl, DIPEA, THF, RT 2h, 86%; *xviii.* KSAc, MeOH, 70°C 5h, 84%; *xix.* HCl, MeOH, 60oC 24h, 78%; *xx.* THF, 55oC 4d, 80%; *xxi.* K2CO3, MeOH, reflux 14h, 88%; *xxii.* NaI, acetone, reflux 4d, 85%; *xxiii.* TMA, THF/DCM/MeOH, RT 3d, 88%

Figure 7: COE SAM Formation by Azide-Alkyne "Click" Reaction

a. Azide-terminated SAM formation using molecule **24**
b. Azide-alkyne "click" reaction with molecule **28**
c. XPS S 2p spectrum following step "*a.*"
d. XPS N 1s spectrum following step "*a.*"
e. XPS N 1s spectrum following step "*b.*" cycloaddition

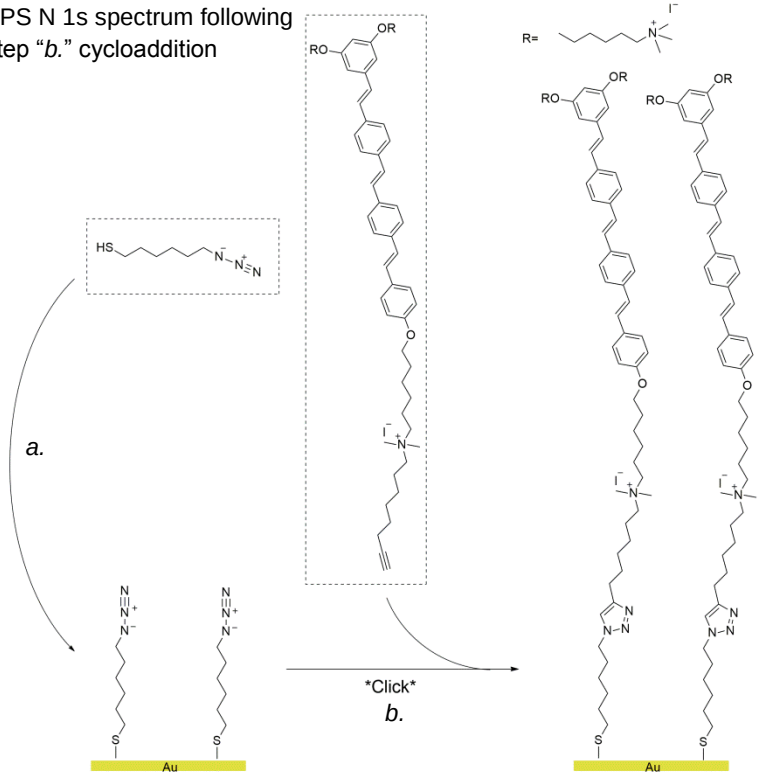

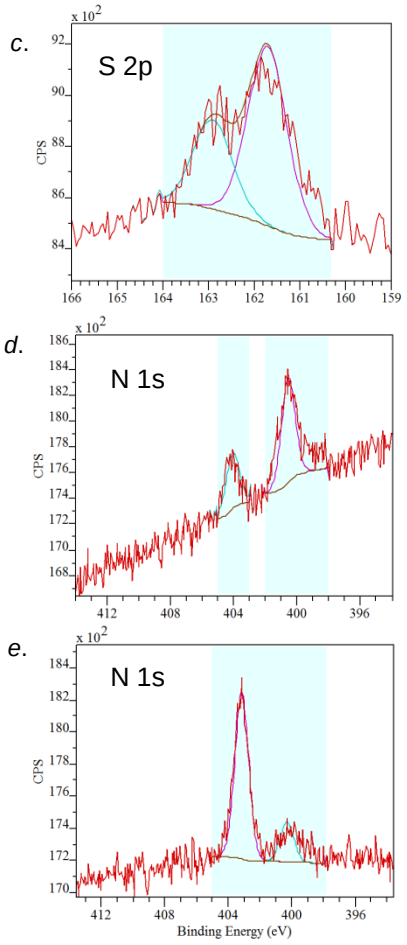

While the two-step SAM formation route continues to be under investigation, there are benefits to having a system where only a single molecular entity is involved (simplified characterization, ability to perform experiments with bacteria in solution, fewer steps involved in SAM-formation). Our attention was thus directed toward completing the synthesis of the thiol-containing COE which had previously stalled when disulfide formation was observed. The mixture of thioacetate-containing COE's and disulfide dimers (molecule **17**) was first treated with hydrochloric acid to remove the acetate protecting groups and afford a mixture of dimers and the free thiol compound. The disulfide bonds were subsequently broken by treating with dithioerythritol. The resulting compound (molecule **19**, shown to the right) was successfully used to functionalize a gold surface. Unlike in previous attempts to form monolayers with a sulfur-containing COE, only the thiolate-gold bond was observed by XPS in the sulfur 2p region (Figure 8). This result demonstrates completion of the first two goals in the way they were originally proposed – the synthesis of a thiol-containing COE and its subsequent use to form a self-assembled monolayer on a gold surface.

Scheme 5:

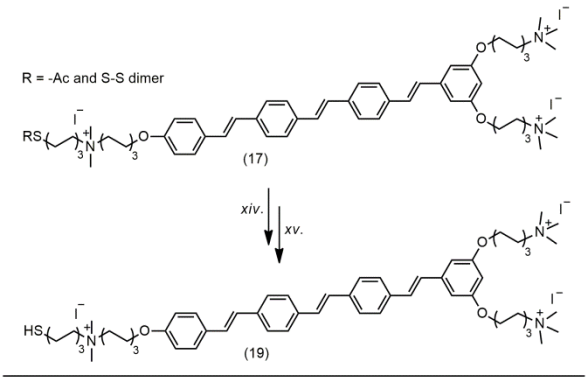

xiv. HCl, MeOH, 40°C 24h, 80%; *xv.* DTE, TEA, MeOH, 40°C 24h

Figure 8: Sulfur 2p Region XPS Spectrum of molecule **19** SAM on gold surface

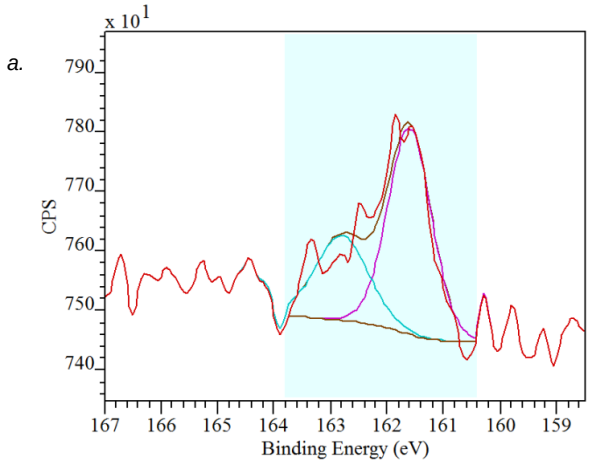

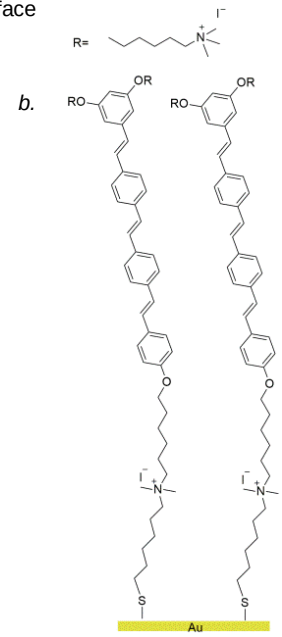

a. SAM of molecule **19** (1mM in MeOH, 18 hours, no stirring)
b. Depiction of molecule **19** SAM on gold

In accordance with the third proposed goal, confocal microscopy was used to confirm the ability of molecule **19** to spontaneously intercalate into bacterial membranes (Figure 9). A culture of *E. coli* was stained with molecule **19** and allowed to sit for thirty minutes before preparing samples for microscopy. The samples were illuminated with light in the range at which molecule **19** absorbs and imaged with a detector tuned to the range at which it fluoresces (see Figure 10). The bright outlines around the cells indicate that fluorescence from molecule **19** is localized to the membranes. Importantly, it has previously been observed that *E. coli* do not autofluorescence in this spectral region.

Figure 9: Confocal Microscopy Images of *E. coli* Stained with Molecule **19**

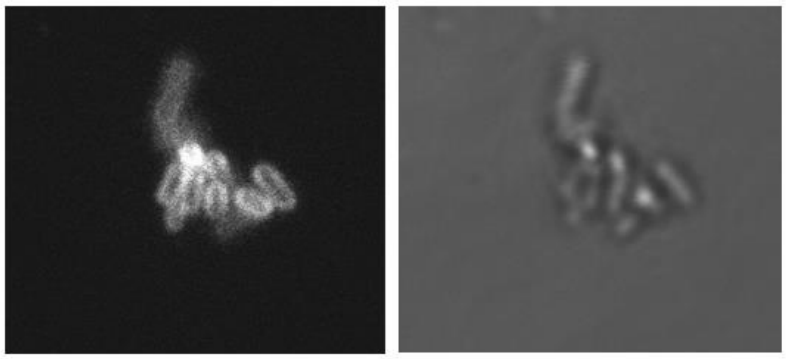

a. Fluorescence image (405nm source, 415-440nm detector)
b. Corresponding bright field image

Figure 10: Absorbance and Fluorescence Spectra of Molecule **19**

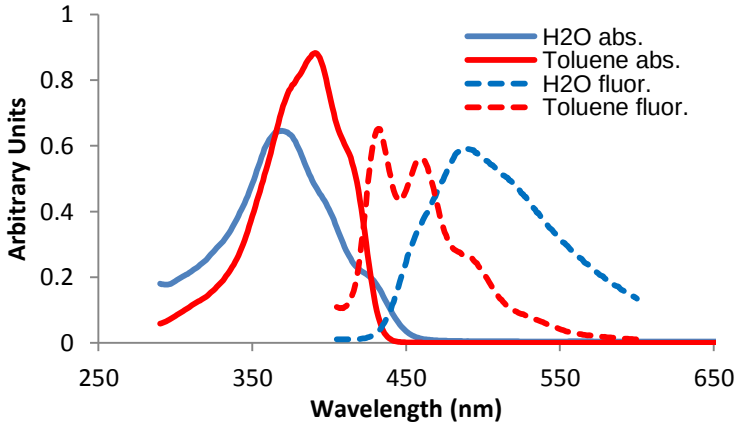

Spectra in toluene were collected using a neutral analogue of molecule **19** in order to simulate the environment inside the cell membrane.

In addition to confocal microscopy, zeta potential and incorporation studies were used to verify the ability of molecule **19** to interact with cell membranes. In both of these experiments, cultures of *E. coli* with known OD_{600nm} were stained with various concentrations of molecule **19**. In the incorporation study, these stained cultures were centrifuged and the absorbance of the supernatant was measured. The amount of molecule **19** incorporated was calculated by subtracting the residual molecule in solution, as measured by absorbance, from the initial concentration. Figure 11 displays the amount of incorporated COE as a function of the initial staining concentration, both in terms of concentration per OD and number of molecules per cell. Zeta potential measurements were used to observe changes in surface

potential of cells with the addition of molecule **19**. As more of the positively-charged COE was added to cell cultures, the more positive (in other words, less negative) the surface of the cells became. The results of both of these studies provide further proof of the ability of molecule **19** to interact with microbial cell membranes.

Figure 11: Incorporation of Molecule **19** as a Function of Concentration

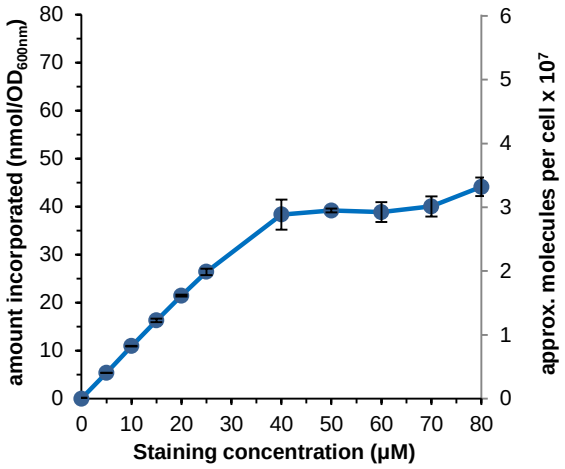

Before attempting to test the ability of the COE monolayer to promote cell adhesion to a gold surface the monolayer coverage was calculated from the XPS spectrum by integrating the Au 4f and S 2p peaks and using published relative sensitivity factors which are considered to be semi-quantitative. This method was also used to calculate the carbon-to-sulfur ratio to ensure that the weak sulfur signal was not significantly affected by background noise. The calculated ratio of approximately fifty carbons per sulfur is in good agreement with the actual ratio in the molecule (46:1). In order to determine the gold-to-sulfur ratio, the percentage of the gold peak which can be attributed to the surface (first atomic layer) was first calculated using the following equation:

Figure 12: Cell Surface Potential as a Function of Molecule **19** concentration

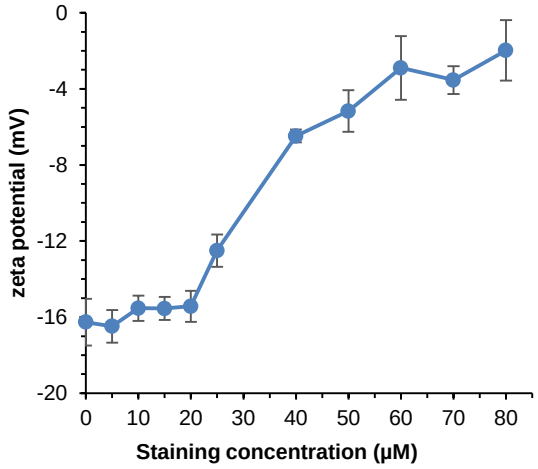

$$P(d) = \exp\left(-d/\lambda\right)$$

where *P(d)* is the probability of an electron escaping from a depth *d* and λ is the mean free path of an electron. For this XPS experiment, it was calculated that an electron from a gold 4f orbital has a MFP of 1.6nm when traveling through bulk gold. It is generally assumed that electrons will not escape from deeper than three or four MFPs and thus this equation was evaluated from the range *d=0* to *d=3.5*. The lattice parameter for gold is approximately 0.4nm which is equivalent to one quarter of a mean free path. The contribution from the first atomic layer was calculated by integrating the equation above between 0 and 0.25 and dividing this value by the integral from 0 and 3.5. The result of this calculation estimates that 16.3% of the gold signal can be attributed to gold atoms within the first atomic layer. Using this value, along with published relative sensitivity factors, the surface coverage was calculated to between 1% (using nitrogen or iodine peaks) to 4% (using sulfur peak) - one COE molecule per 25-100 gold atoms.

If it is assumed that a bacterial cell has a surface contact area of $1um^2$, and given that there are approximately 6 million gold atoms in that area, one surface-bound cell has the potential to interact with 240,000 COE molecules (using the 4% coverage calculated by XPS). As the strength of cell-COE interactions is not known, no minimum value for surface attachment can be hypothesized. It is worth noting that MFC experiments using COEs in solution are typically run at a concentration such that there are 1-5e6 COE molecules per cell.

Scanning electron microscopy analysis seems to indicate that such a sparse coverage has no effect on the ability of *Shewanella oneidensis* to attach to the surface. In these experiments, the functionalized surface substrate as well as a bare substrate (gold on glass) were incubated overnight with a liquid culture of *S. oneidensis*. Substrates were vortexed and washed with PBS buffer to remove unattached cells. Cells were fixed and dried with formalin and ethanol and counted using SEM. The average substrate area per cell was found to be $1324um^2$ and $1259um^2$ for the unfunctionalized and functionalized substrates respectively.

It is reasonable to assume that a certain minimum surface coverage is required in order to observe a significant difference in cell adhesion. In order to increase the surface coverage, the conditions for SAM formation were changed (1mM in water instead of methanol, three days instead of 18 hours, and stirred instead of static). The changes in conditions led to a five-fold increase in coverage based on XPS results. Given the physical structure of the COE molecule, this is likely approaching the upper limit for surface coverage.

Due to the large variability in calculated coverage depending on which element is used in the calculation, a second method was used to validate the XPS results. Reductive desorption of thiol monolayers on gold is well established in the literature and has been used to calculate SAM coverages. A coiled gold wire with a $1cm^2$ surface area was functionalized in a similar manner to the gold films used in the XPS studies. Cyclic voltammetry was used to reduce the thiolate-gold bonds by sweeping between 0 and -1.4V in a supporting electrolyte solution consisting of 10mM NaOH. The total charge, and thus the number of electrons associated with this reduction was determined by integrating under the curve. As this is known to be a one-electron event, the total number of electrons is analogous to the total number of thiolate-gold bonds reduced over the entire $1cm^2$ surface. From the cyclic voltammogram shown in figure 13, a coverage of 7%, or one COE per fourteen gold atoms, was calculated.

FIGURE 13: Reduction of COE SAM by CV

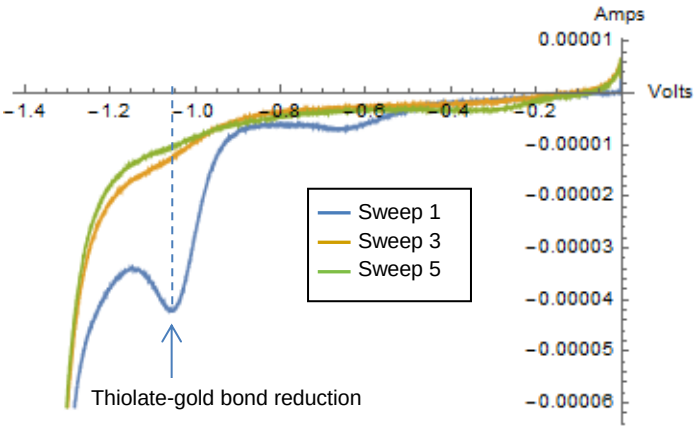

A substrate with the higher degree of COE SAM coverage (~10%) and a bare substrate were subjected to the same cell adhesion experiment described previously except the substrates were not vortexed during cleaning. Instead, the substrates were simply washed under a stream of PBS buffer in order to remove only the most weakly adhered cells. SEM micrographs were collected at 1mm intervals across the center of the substrates and the cells in each frame were counted. Figure 14 displays the cell counts as averages per 7000um^2 micrograph frame. The large deviation may be attributable to non-uniform cell coverage which resulted from the manner in which the cultures were stirred. As the center of the electrode experienced less shear force than the edges, more cells may have been able to settle further from the edges. This issue was partially mitigated by ensuring that micrographs were collected in identical positions on the functionalized and control substrates. While efforts are underway to eliminate this issue, it is unlikely that it had any influence on the conclusions that can be drawn from the data presented in Figure 13. One of the micrographs used for the cell coverage experiment, as well as a magnified image can be found in Figure 15. Unlike the previous adhesion study, the difference in adhesion between the bare gold and the 10% coverage COE SAM is statistically significant (p = 0.011). This result demonstrates the ability of a COE SAM to promote cell adhesion to a gold surface.

Figure 14: Cell Counts from SEM Analysis of Bare Substrate and 20% Coverage COE SAM

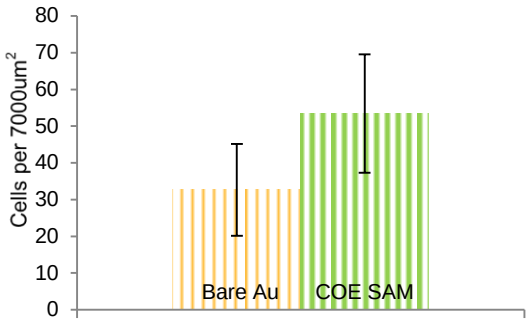

Figure 15: SEM Micrographs of *S. oneidensis* on 20% Coverage COE SAM

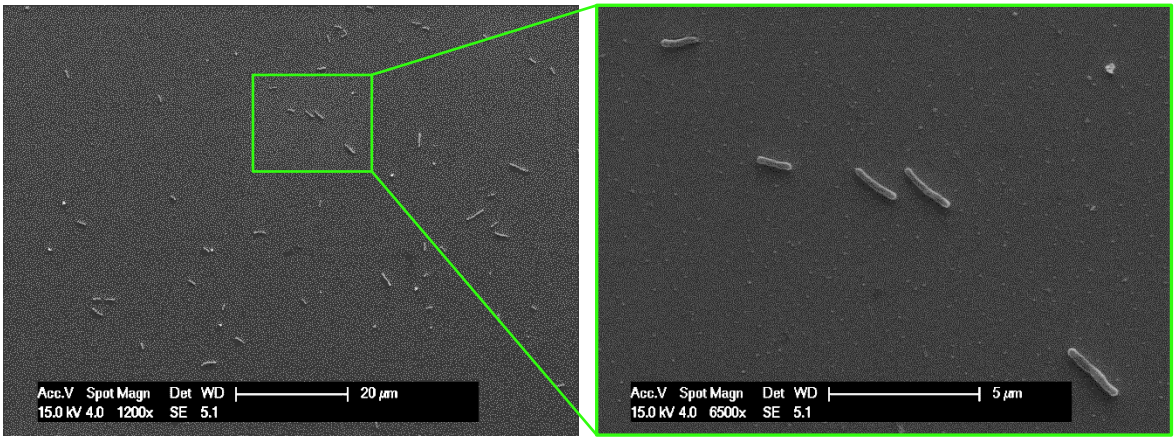

The preceding experiments and results have demonstrated the successful completion of the first four goals outlined for this project. The fifth goal is the direct application of these positive results to bioelectrochemical systems. Much of this work was accomplished through close collaboration with James Sumner at ARL, who is an expert in this field. During a month-long visit to ARL, a student from this group worked closely with a resident post doc in Jim Sumner's group.

A typical U-tube setup for measuring current generation is depicted in Figure 16. Under anaerobic conditions, bacteria grow and respire on the working electrode. To test the ability of the COE SAMs to enhance electronic communication at the abiotic-biotic interface, U-tube microbial fuel cells were constructed with gold anodes (either bare or functionalized). As a model organism, *Shewanella oneidensis* was selected due to its exoelectrogenic abilities but relative difficulty in utilizing gold as a terminal electron acceptor.

Figure 16: COE SAM Electrode Incorporated in Typical U-Tube Microbial Fuel Cell

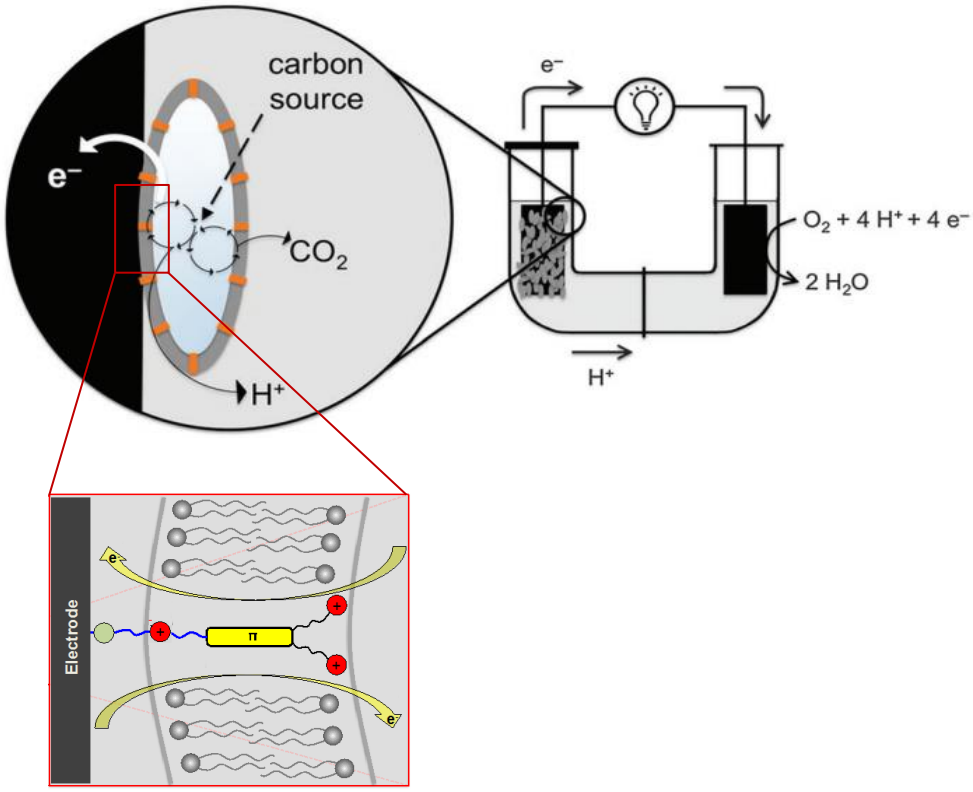

The results of the microbial fuel cell experiments conducted at ARL can be seen in Figure 17. The discontinuities in the voltage-versus-time plot are points at which the external resistance was swept in order to generate polarization curves. An increase of 27% in peak voltage was

Figure 17: U-Tube MFC Voltage Output and Polarization Curve

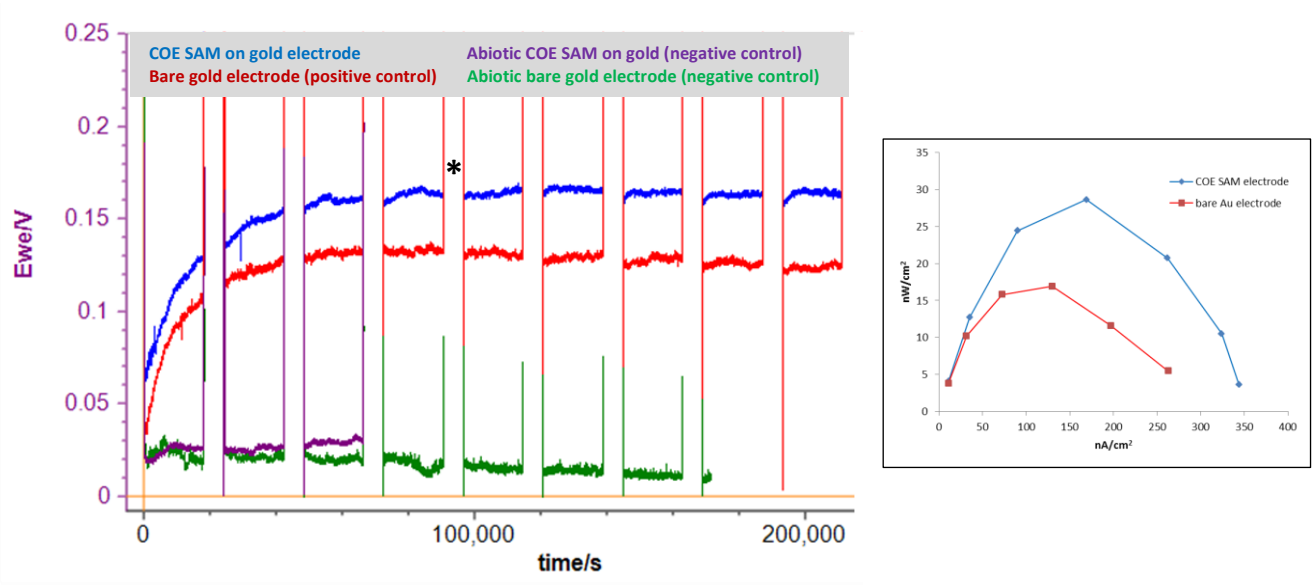

* denotes the resistance sweep that was used to generate the polarization curve shown to the right

observed when the anodes were functionalized with a COE monolayer. This increased voltage was sustained for the duration of the experiment (>56 hours). Importantly, in the absence of cells, no additional voltage was measured with COE SAM functionalized anodes relative to bare gold anodes (approximately 0V in both cases). From the polarization curve in Figure 17, it is apparent that the surface functionalization increased peak power – a result indicative of reduced internal resistance, most likely at the abiotic-biotic interface.

The successful completion of all five key project milestones has been achieved. A surface-binding COE was designed and synthesized. The molecule was shown to form monolayers on gold surfaces and the conditions for monolayer formation were optimized. The molecule, when added in solution, was successfully incorporated into microbial membranes. Enhancement of physical interactions between microbes and a functionalized anode was observed. Finally, improved electronic communication at the abiotic-biotic interface was confirmed by voltage output and polarization curves collected from U-tube microbial fuel cells. The results of this STIR project are currently being prepared for publication. In addition, further optimization of the described methods is underway at UCSB and ARL.